International Journal of Electrical and Electronic Engineering & Telecommunications

ISSN 2319 – 2518 www.ijeetc.com
Special Issue, Vol. 1, No. 1, March 2015
National Level Technical Conference P&E- BiDD-2015

Research Paper

SENSORLESS AND TRANSDUCERLESS CONTROL OF PERMANENT MAGNET BRUSHLESS DC MOTOR USING DIRECT BACK EMF DETECTION

N Muraly[1]*

*Corresponding Author: N Muraly, ✉ nmlect@gmail.com

This paper deals with a scheme of permanent magnet brushless dc motor drive sensor less speed control. The simulation model of BLDC motor is obtained by approximation of real back EMF wave form to ideal trapezoidal waveform. A sensor less control of BLDC motor requires a three-phase inverter with six-step commutation. These commutation timing is determined by the rotor position, at every 600 by detecting zero crossing of back EMF on the floating coil of the motor. Encouraging simulation results have been obtained.

Keywords: Permanent magnet brushless DC motor, Speed sensorless control, Rotor position detection, Back EMF

INTRODUCTION

Permanent magnet brushless motors drives is a topic of active research, due to their high power density and ease of control (Jianwen Shao *et al.*, xxxx; and Johnson, 1999). The brushless motors are generally controlled using a three-phase power semiconductor bridge (GE US Patent No. 4654566). The BLDC motor requires a rotor position sensor for starting and providing proper commutation sequence to turn on the power devices in the Inverter Bridge (Lizuka *et al.*, 1985).

The position sensors such as resolvers, absolute position encoders, and Hall sensors increase cost and size of the motor. A special mechanical arrangement needs to be made for mounting the sensors. These sensors limiting the operation of motor, the resolvers need special external circuit to obtain the correct position information (Rajashekara *et al.*, 1996; and Matsui, xxxx). Due to these limitations of motor operation with position sensors, sensorless operation of PM brushless motors is receiving wide attention (Jufer and Osseni, 1985; and Chan *et al.*, 1995).

A BLDC motor with the characteristics of high speed and high power density has been

[1] Faculty of Engineering, University Malaysia Sarawak (UNIMAS), Kota Samarahan 94300, Sarawak, Malaysia.

more widely used in high performance drives (Krishnan, 1986). The torque and speed characteristic of BLDC motor is very important factor in the design of motor drive system, so it is necessary to predict the precise value of torque which is determined by the waveform of back EMF. The conventional simulation model of BLDC motor is obtained by approximation of real back EMF wave form to ideal trapezoidal waveform. But, as the shapes of slot skew and magnet of BLDC motor varies subject to design purposes, the real back EMF waveform is at some degree deviated from the ideal trapezoidal waveform. As a result when using the ideal trapezoidal waveform, the error occurs. In consequence, in order to lesson such an error, the model of BLDC motor with real back EMF waveform is needed instead of its approximation model (Pillay and Krishnan, 1989).

This paper describes in detail the simulation of permanent magnet brushless dc motor drive sensorless speed control. The reduction of error in simulation, a simulation model of BLDC motor with nearly real back emf waveform is proposed. Section II briefly describes the Modelling of BLDC Motor and Section III deals with the Back EMF detection. Section IV details the simulation results of Sensorless BLDC Motor. Section V has the conclusion and future research on the subject.

MODELING OF PMBLDC MOTOR DRIVE SYSTEM

BLDC drive consists of a three-phase current controlled voltage source inverter (CRPWM), the motor and controller. The inverter, which is connected to the dc supply, feeds controlled power to the motor. And frequency of the inverter output voltage depends on the six switching signals, which are generated by the controller. The state of these switching signals at any instant is determined by the rotor position, speed error and the feedback currents. The controller synchronizes the drive and maintains the motor speed at the reference value even during load and supply fluctuations. In the inverter block models the IGBT based three-phase voltage source inverter. Three phase stator currents are synchronized with the rotor position by providing proper gating signals to the devices of the inverter. The reference value of a phase current is determined by the position of the rotor and motor phase current are used to find the voltage of that phase as given below.

$$If\,(i_a*+Hb) \geq i_a \text{ then } S_a = 1 \text{ else } S_a = 0 \quad ...(1)$$

$$If\,(i_b*+Hb) \geq i_b \text{ then } S_b = 1 \text{ else } S_b = 0 \quad ...(2)$$

$$If\,(i_c*+Hb) \geq i_c \text{ then } S_c = 1 \text{ else } S_c = 0 \quad ...(3)$$

$$v_{as} = \frac{v_{dc}}{3}(2S_a - S_b - S_c) \quad ...(4)$$

$$v_{bs} = \frac{v_{dc}}{3}(2S_b - Sa - S_c) \quad ...(5)$$

$$v_{cs} = \frac{v_{dc}}{3}(2S_c - S_b - S_c) \quad ...(6)$$

where *Hb* is the Hystersis band S_a, S_b and S_c are switching function *s*(which are either 1 or 0). V_a, V_b and V_c are the phase voltages of inverter and V_{dc} is the *dc* link voltage.

The derivation of this model is based on the assumptions that the induced currents in the rotor due to stator harmonic fields are neglected and that iron and stray losses are also neglected. Damper windings are not usually a part of the PMBDCM, damping is provided by the inverter control. The motor is considered to have three phases, even though the derivation procedure is valid for any number of phases. The coupled circuit equations of the stator windings in terms of motor electrical constants are:

$$\begin{bmatrix} v_{as} \\ v_{bs} \\ v_{cs} \end{bmatrix} = \begin{bmatrix} R_s & 0 & 0 \\ 0 & R_s & 0 \\ 0 & 0 & R_s \end{bmatrix} \begin{bmatrix} i_{as} \\ i_{bs} \\ i_{cs} \end{bmatrix} + \begin{bmatrix} L_{aa} & L_{ab} & L_{ac} \\ L_{ba} & L_{bb} & L_{bc} \\ L_{ca} & L_{cb} & L_{cc} \end{bmatrix} + \begin{bmatrix} i_{as} \\ i_{bs} \\ i_{cs} \end{bmatrix} + \begin{bmatrix} e_{as} \\ e_{bs} \\ e_{cs} \end{bmatrix} \quad ...(7)$$

where R_s is the stator resistance per phase, assumed to be equal for all three phases. The induced e_{mfs}, e_{as}, e_{bs}, and e_{cs} are all assumed to be trapezoidal, as shown in Figure 1, where E_p is the peak value, derived as:

$$E_p = {}^{a}{}_{p}\mu_m \quad ...(8)$$

where μ_{mi} is the angular velocity and ${}^{a}{}_{p}$ in the flux linkages of rotor magnet.

If there is no change in the rotor reluctance with angle because of a non-salient rotor, assuming three symmetric phases, the following are obtained.

$L_{aa} = L_{bb} = L_{cc} = L$; and $L_{ab} = L_{ba} = L_{ac} = L_{ca} = L_{bc} = L_{cb} = M(H)$ ...(9)

The PMBDCM model is:

$$\begin{bmatrix} v_{as} \\ v_{bs} \\ v_{cs} \end{bmatrix} = \begin{bmatrix} R_s & 0 & 0 \\ 0 & R_s & 0 \\ 0 & 0 & R_s \end{bmatrix} \begin{bmatrix} i_{as} \\ i_{bs} \\ i_{cs} \end{bmatrix} + \begin{bmatrix} L & M & M \\ M & L & M \\ M & M & L \end{bmatrix} p \begin{bmatrix} i_{as} \\ i_{bs} \\ i_{cs} \end{bmatrix} + \begin{bmatrix} e_{as} \\ e_{bs} \\ e_{cs} \end{bmatrix} \quad ...(10)$$

The stator phase currents are constrained to be balance, i.e., $I_{as} + I_{bs} + I_{cs} = 0$, which leads to the simplification of the inductance matrix in the model as:

$$\begin{bmatrix} v_{as} \\ v_{bs} \\ v_{cs} \end{bmatrix} = \begin{bmatrix} R_s & 0 & 0 \\ 0 & R_s & 0 \\ 0 & 0 & R_s \end{bmatrix} \begin{bmatrix} i_{as} \\ i_{bs} \\ i_{cs} \end{bmatrix} + \begin{bmatrix} L-M & 0 & 0 \\ 0 & L-M & 0 \\ 0 & 0 & L-M \end{bmatrix} p \begin{bmatrix} i_{as} \\ i_{bs} \\ i_{cs} \end{bmatrix} + \begin{bmatrix} e_{as} \\ e_{bs} \\ e_{cs} \end{bmatrix} \quad ...(11)$$

The electromagnetic torque is given by

$$T_e = [e_{as}i_{as} + e_{bs}i_{bs} + e_{cs}i_{cs}]\frac{1}{\mu_m} \quad ...(12)$$

The instantaneous induced emfs can be written from Figure 4.1 and equation can be written as:

$$e_{as} = f_{as}(\bar{}_r)\,{}^{a}{}_{p}\mu_m \quad ...(13)$$

$$e_{bs} = b_{bs}(\bar{}_r)\,{}^{a}{}_{p}\mu_m \quad ...(14)$$

$$e_{cs} = f_{cs}(\bar{}_r)\,{}^{a}{}_{p}\mu_m \quad ...(15)$$

where the functions = $f_{as}(\bar{}r)$, $f_{bs}(\bar{}r)$ and $f_{cs}(\bar{}r)$ have the same shpes as e_{as}, e_{bs} and e_{cs} with a maximum magnitude of + or –1.

$$f_{as}(\bar{}_r) = 1 \quad 0^0 < \bar{} \le 120 \quad ...(16)$$

$$f_{as}(\bar{}_r) = \frac{6}{®}(® - \bar{}) - 1 \quad 120^0 < \bar{} \le 180^0 \quad ...(17)$$

$$f_{as}(\bar{}_r) = -1 \quad 180^0 < \bar{} \le 300^0 \quad ...(18)$$

$$f_{as}(\bar{}_r) = \frac{6}{®}(\bar{} - 2®) + 1 \quad 300^0 < \bar{} \le 360^0 \quad ...(19)$$

The function of rotor position ($\bar{}$) and fas ($\bar{}r$) is defined as:

$$T_e = {}^{a}{}_{p}[f_{as}(\bar{}_r)i_{as} + f_{bs}(\bar{}_r)i_{bs} + f_{cs}(\bar{}_r)i_{cs}] \quad ...(20)$$

The equation of the motion for a simple system with inertia J, friction coefficient B, and load torque T_1 is:

$$J\frac{d\mu_m}{dt} + B\mu_m = (T_e - T_L) \qquad \text{...(21)}$$

The electrical rotor speed and position are related by

$$\frac{d\bar{\ }_r}{dt} = \frac{P}{2}\mu_m \qquad \text{...(22)}$$

Sensorless Control of BLDC Motor

The drive system is dependent on the position and current sensors for control. Elimination of both types of sensors is desirable in fuel pump, hybrid electric vehicle and fan drives. The position sensor requires a considerable labour and volume in the motor for its mounting. That makes it all the more important to do without the position sensor for the control of the PMBLDC drive systems.

Enhanced Sensorless Algorithms

The induced emf can be sensed form the machine model by using the applied currents and voltages and machine parameters of resistance, self-inductance, and mutual inductance. The advantage of this method is that an isolated signal can be extracted; because the input currents and voltages are themselves isolated signals. The voltages can be extracted from the base or gate dries signal and the dc-link voltage. The variations in the dc-link voltage can be estimated form the dc-link filter parameters and the dc-link current parameter sensitivity, particularly that of the stator resistance, will introduce an error in the induced emf estimation, resulting in inaccurate commutation signal to the inverter. Sensing coils in the machine can be installed inexpensively to obtain induced-emf signals. The advantages of this method are that the signal are fairly clean, parameter-insensitive and galvanically isolated. The disadvantages are in the additional manufacturing process and additional wire harness forms the machine. The latter is not acceptable in refrigerator compressor motor drives, because of hermetic sealing requirements.

DIRECT BACK EMF DETECTION

A three-phase inverter with six-step commutation drives the Brushless DC (BLDC) motors. The commutation phase sequence is like AB-AC-BC-CA-CB. Each conducting phase is called one step. The conducting interval for each phase is 120 electrical degrees. Therefore, only two phases conduct current at any time. Leaving the third phase floating. In order to produce maximum torque, the inverter should be commutated every 60° so that current is in phase with the back EMF. The commutation timing is determined by the rotor position, which can be determined every 60° by detecting zero crossing of back EMF on the floating coil of the motor.

The noisy motor neutral point causes problems for the sensorless system. The proposed back EMF detection is trying to avoid the neutral point voltage. If the proper PWM strategy is selected, the back EMF voltage referred to ground can be extracted directly from the motor terminal voltage. For BLDC drive, only two out of three phases are excited at any instant of time.

The PWM drive signal can be arranged in three ways:

- On the high side: the PWM is applied only on the high side switch, the low side is on during the step.
- On the low side: the PWM is applied on the low side switch, the high side is on during the step.
- On both sides: the high side and low side are switched on/off together.

In the proposed scheme, the PWM signal is applied on high side switches only, and the back EMF signal is detected during the PWM off time. Figure 1 shows the concept detection circuit. Assuming at a particular step, phase A and B are conducting current, and phase C is floating. The upper switch of phase A is controlled by the PWM and lower switch of phase B is on during the whole step. The terminal voltage Vc is measured. Figure 2 showsthe PWM signal arrangement. Figure 3 Circuit model of proposed Back EMF detection during the PWM off time moment.

Figure 1: Back EMF Zero Crossing Detection Scheme

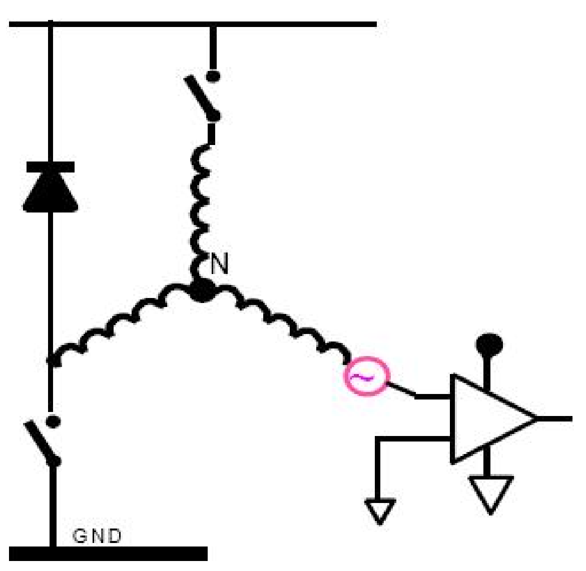

Figure 2: PWM Strategy for Direct Back EMF Detection Scheme

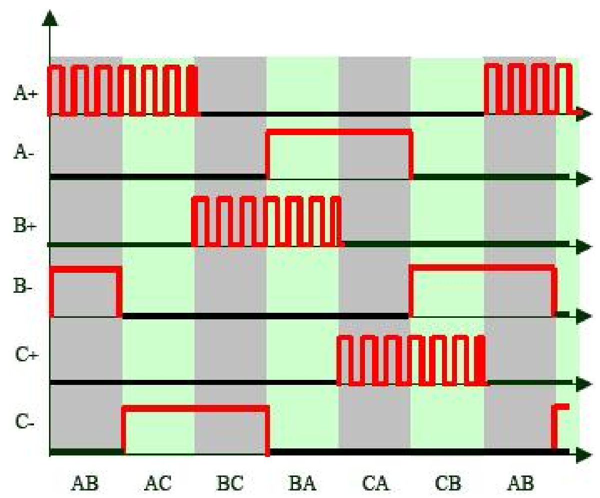

Figure 3: Circuit Model of Proposed Back EMF Detection During the PWM Off Time Moment

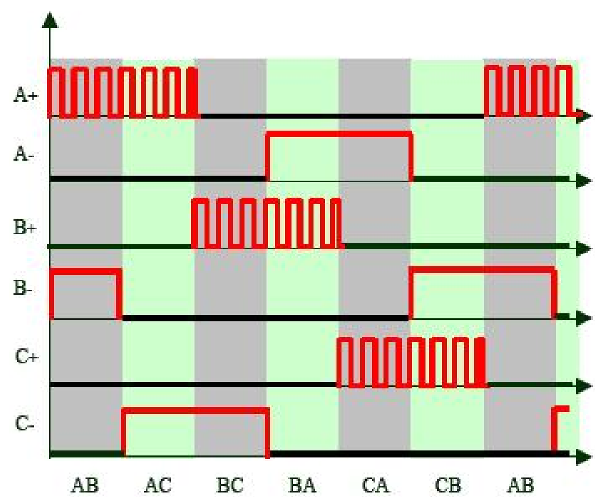

When the upper switch of phase A is turned on, the current is flowing through the switch to winding A and B. When the upper transistor of the half bridge is turned off, the current freewheels through the diode paralleled with the bottom switch of phase A. During this freewheeling period, the terminal voltage vc is detected as Phase C back EMF when there is no current in phase C.

From the circuit, it is easy to see $v_c = e_c + v_n$, where v_c is the terminal voltage of the floating phase C, e_c is the phase back EMF and v_n is the neutral voltage of the motor.

From phase A, if the forward voltage drop of the diode is ignored, we have

$$V_n = 0 - ri - L\frac{di}{dt} - e_a \quad ...(23)$$

From phase B, if the voltage drop on the switch is ignored, we have

$$V_n = ri + L\frac{di}{dt} - e_b \quad ...(24)$$

$$V_n = -\frac{e_a + e_b}{2} \quad ...(25)$$

Assuming a balanced three-phase system, if we ignore the third harmonics, we have

$$e_a + e_b + e_c = 0 \quad ...(26)$$

Or, if we don't ignore the third harmonics, we will have

$$e_a + e_b + e_c = e_3 \quad ...(27)$$

where e_3 is the third harmonics.

Let's first finish the analysis without considering the third harmonics.

From (25) and (26),

$$V_n = \frac{e_c}{2} \quad ...(28)$$

So, the terminal voltage V_c,

$$V_c = e_c + V_n = \frac{3}{2}e_c \quad ...(29)$$

From the above equations, it can be seen that during the off time of the PWM, which is the current freewheeling period, the terminal voltage of the floating phase is directly proportional to the back EMF voltage without any superimposed switching noise. It is also important to note that this terminal voltage is referred to the ground instead of the floating neutral point. So, the neutral point voltage information is not needed to detect the back EMF zero crossing, and we don't need to worry about the common mode voltage. Since the true back EMF is extracted from the motor terminal voltage, the zero crossing of the phase back EMF can be detected very precisely.

If we consider the third harmonics, from (25) and (28),

$$v_n = \frac{e_c}{2} - \frac{e_3}{2} \quad ...(30)$$

So, the terminal voltage V_c,

$$Vn = e_c + V_n = \frac{3}{2}e_c - \frac{e_3}{2} \quad ...(31)$$

Therefore, the terminal voltage will see the third harmonics. However, since the zero crossing of the fundamental wave will coincide with the zero crossing of the third harmonics, the third harmonic won't affect the zero crossing of the fundamental wave.

SIMULATION RESULTS

Simulation results of entire BDCM drive system are presented in this section. PMBDCM model in abc phase variables is used in this simulation. Further an ideal model with zero conduction voltage drops and zero switching time is utilized in this simulation for the switches and diodes. The operational modes determine whether one phase or two phases conduct at a given time. The turn-on and turn-

Figure 4a: Different Speed Range at Half Load Torque

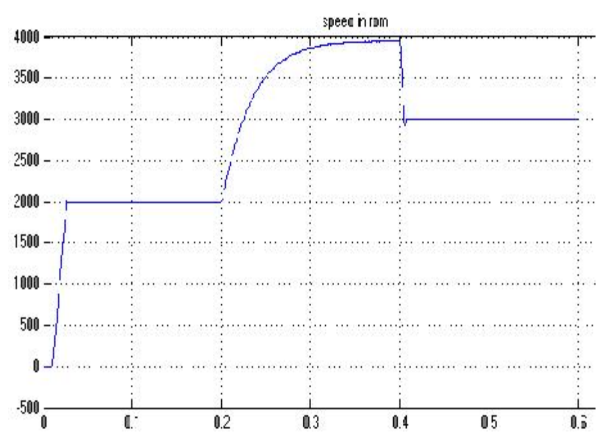

Figure 4b: Total Developed at Half Load Torque

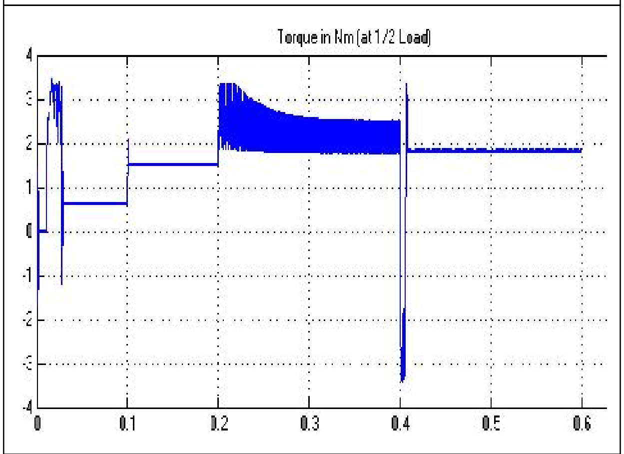

Figure 4c: Phase Current Ia at Half Load Torque

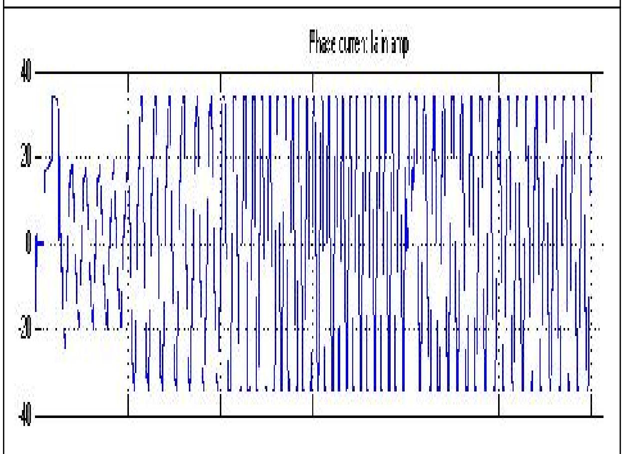

Figure 4d: Back EMF of Phase A at Half Load Torque

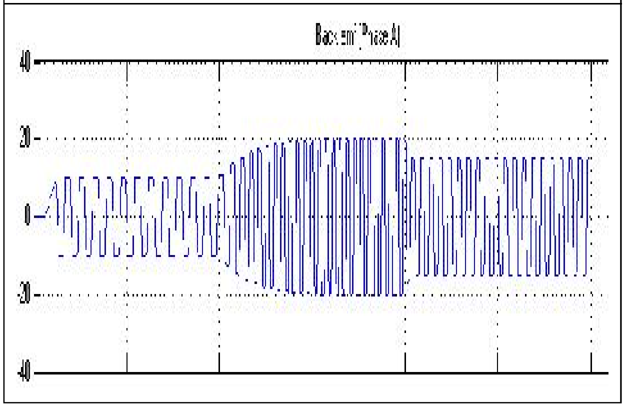

of times of the power devices are neglected. The Speed and Torque Curves with Various Load is shown in Figure 4.

Figure 4 simulated for half of the rated toque. Speed refecrences given at 0.01 sec

Figure 5a: Speed Curve at ½ Load Torque

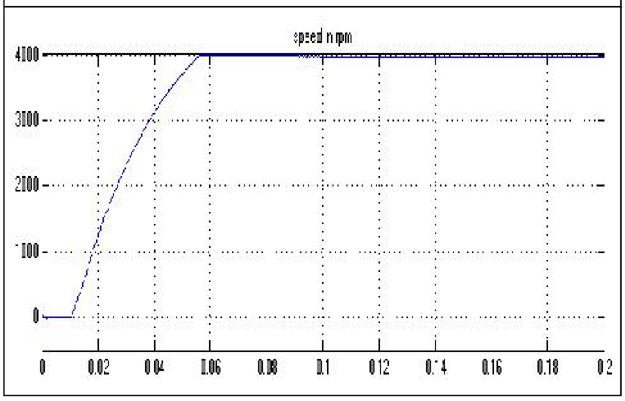

Figure 5b: Phase Current Waveform at ½ Load Torque

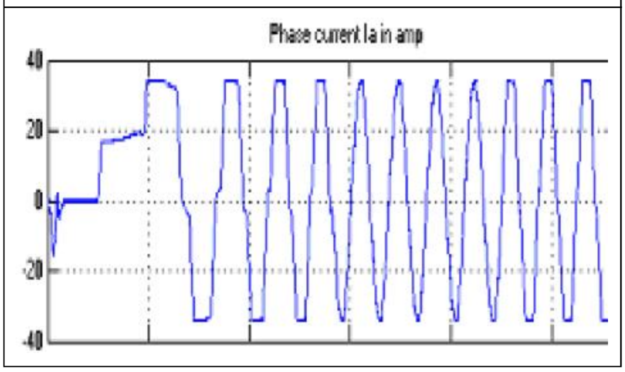

Figure 5c: Phase Current Waveform at Full Load Torque

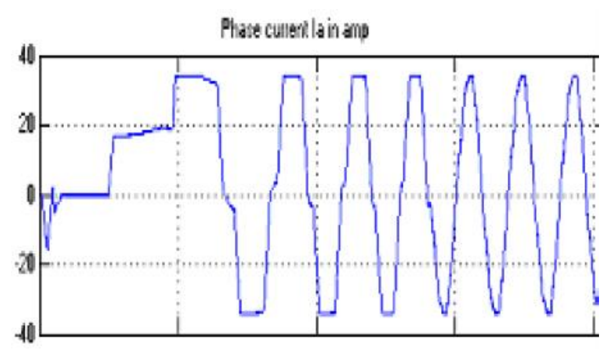

for 2000 rpm, 0.2 sec for 4000 rpm, and 0.4 sec for 3000 rpm.

Figure 5 is simulated at 4000 rpm. Speed reference given a 0.01 sec, load torque is given at 0.09 sec.

Figure 6a: Shows the Speed Curve at ½ Load Torque

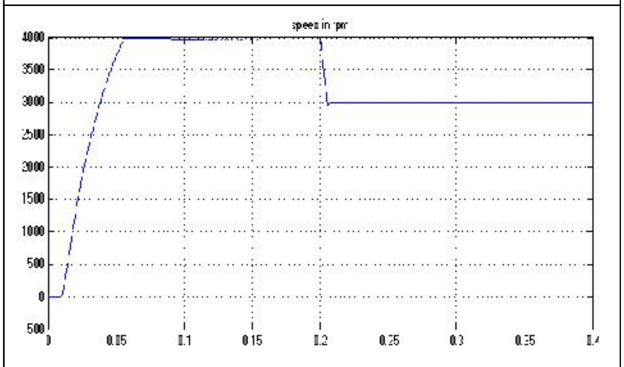

Figure 6b: Shows the Torque at ½ Load Torque

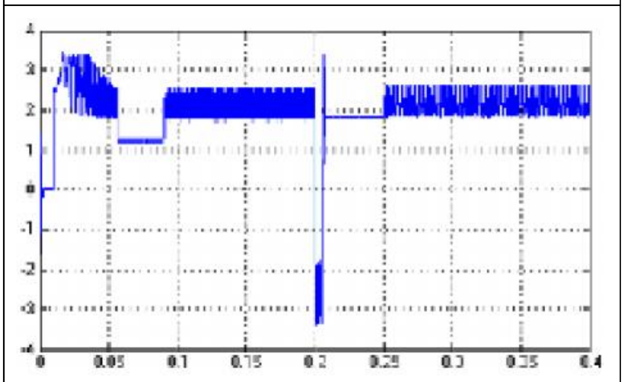

Figure 6c: Shows the Current ½ Load Torque

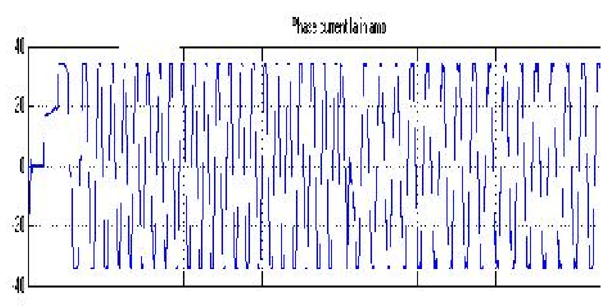

Figure 6 simulated for Speed reference given at 0.01 sec for 4000 rpm, 0.2 sec for 1000 rpm, and 0.4 sec for 3000 rpm. Also, load torque is given at 0.09 sec for ½ load and 0.25 sec at full load.

Figure 7 simulated for Speed reference for 4000 rpm. Also, load torque is given at 0.05

Figure 7a: Speed Curve at Various Load Torque Values

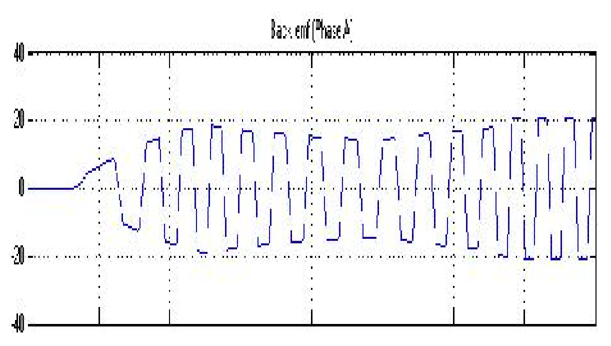

Figure 7b: Developed Torque Curve at Various Load Torque

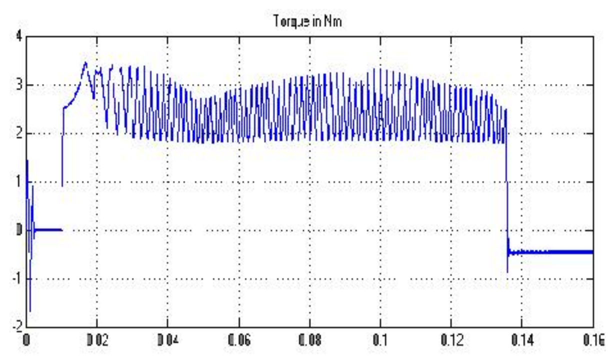

Figure 7c: Back EMF Curve at Various Load Torque

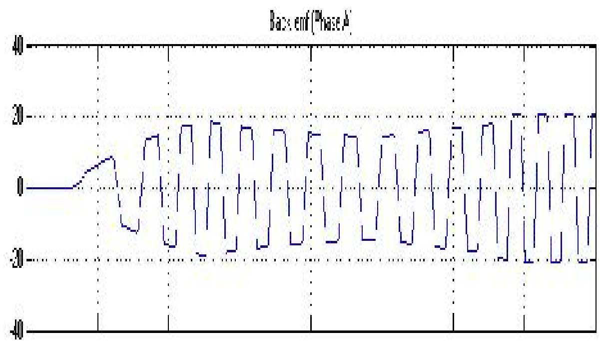

sec for, full load and 0.25 sec at half load and no load torque at 0.13 sec.

Every instance of a power device turning on or off was simulated to calculate the current oscillations and resulting torque pulsations. The relationship between the commutation-induced toque pulsation and the current being commutated is linear. The frequency of the commutation-induced toque pulsations increase as the number of poles of the machine is increased, thus reducing their effects on the speed. A high pole number is therefore advantageous in a speed servo. The numbers of pulsations increase with an increase in the number of poles for a given mechanical rotation, a very high pole number undesirable for position servo performance.

CONCLUSION

Sensorless Permanent magnet brushless motors drives have been implemented and tested using Matlab/Simulink. PMBDCM model in ABC phase variables is used in this simulation. Further an ideal model with zero conduction voltage drops and zero switching time is utilized in this simulation for the switches and diodes. The operational modes determined whether one phase or two phases conduct at a given time. The Simulation results for sensorless PMBLDC drives have been presented. The influence on variations of loads with different speed reference has been studied and reported.

REFERENCES

1. Chan C C, Liang J Z and Xis W (1995), "Novel Wide Range Speed Control of Permanent Magnet Brushless Motor Drives", *IEEE Transaction on Power Electronics*, Vol. 10, September, pp. 539-546.
2. "Control System Method Operating an Electronically Commutated Motor and Laundering Apparatus", Granted to GE US Patent No. 4654566.
3. Jianwen Shao, Dennis Nolan and Thomas Hopkins, "A Novel Direct Back EMF Detection for Sensorless Brushless DC Motor Drives", *IEEE Transactions on Power Electronics Drives*.
4. Johnson J (1999), "Review of Sensorless Methods for Brushless DC", *IAS Annual Meeting*, pp. 143-150.
5. Jufer M and Osseni R (1985), "Back EMF Indirect Detection for Self-Commutation of Synchronous Motor in Proceeding", pp. 7441-7447.
6. Krishnan R (1986), "Selection Criteria for Servo Motor Drives", in Proceedings IEEE IAS Annual Meeting, pp. 301-308.
7. Lizuka K, Usuhashi H, Kano M, Endo T and Mohri K (1985), "Micro Computer Control for Sensorless Brushless Motor", *IEEE Transaction on Industrial Applications*, Vol. 21, May/June, pp. 595-601.

8. Matsui N, "Sensorless Operation of Brushless DC Motor Drives, IEEE IECON'93 Proceeding, pp. 739-744.

9. Pillay P and Krishnan R (1989), "Modeling, Simulation and Analysis of Permanent Magnet Motor Drives: Part II, The Permanent Magnet Brushless Motor Drives", *IEEE Transactions on Power Electronics*, April.

10. Rajashekara K, Kawamura A and Matsuse K (1996), "Sensorless Control of AC Motor Drives, Speed and Position Sensorless Operation", IEEE Press, New York.

APPENDIX

Nomenclature	
K_b	Back emf constant
K_t	Torque constant
μ_{ref}	Reference speed
v_r	Converter Input Voltage/phase
R	Resistance of the winding
L, M	Self and Mutual inductance of the winding
–	Rotor angle
¦	Efficiency